



High-frequency ultrasound shear wave dispersion imaging for male infertility: a pilot study

Shijun Zhang^{1#}, Mingtai Wu^{1#}, Li Xu¹, Hongxiang Wang², Lixin Jiang¹

¹Department of Ultrasound, Renji Hospital, School of Medicine, Shanghai Jiao Tong University, Shanghai, China; ²Department of Andrology, Renji Hospital, School of Medicine, Shanghai Jiao Tong University, Shanghai, China

Contributions: (I) Conception and design: L Jiang; (II) Administrative support: L Jiang; (III) Provision of study materials or patients: H Wang; (IV) Collection and assembly of data: S Zhang, M Wu, L Xu; (V) Data analysis and interpretation: S Zhang, M Wu; (VI) Manuscript writing: All authors; (VII) Final approval of manuscript: All authors.

[#]These authors contributed equally to this work.

Correspondence to: Lixin Jiang, MD. Department of Ultrasound, Renji Hospital, School of Medicine, Shanghai Jiao Tong University, No. 160 Pujian Rd., Shanghai 200127, China. Email: jinger_28@sina.com.

Background: The characteristics of testicular viscoelasticity could help identify azoospermia. This study sought to assess the diagnostic value of viscoelasticity for male infertility using high-frequency ultrasound shear wave dispersion (SWD) imaging.

Methods: In this prospective study, 330 consecutive patients with male infertility were allocated to the ultrasound normal group, the varicocele group, the non-obstructive azoospermia (NOA) group, and the obstructive azoospermia (OA) group, and 30 healthy volunteers were allocated to the control group. Two physicians with over 10 years of experience each in andrology ultrasound measured the viscosity coefficient, dispersion slope, and elasticity of each testis, respectively. The testicular viscoelasticity was compared among the patients from the four groups and the control group. The inter-reader variability between the two physicians was assessed. The diagnostic efficacy of viscoelasticity for NOA was evaluated by receiver operating characteristic (ROC) curve analysis. Binary logistic regression was used to analyze the risk factors for NOA.

Results: Among the 360 participants, the viscosity coefficient, dispersion slope, and elasticity were all higher in the NOA group than the other groups ($P < 0.001$). The inter-reader variability was excellent [intraclass correlation coefficient (ICC): 0.87–0.96]. Comparisons between the patient groups categorized by testicular volume (TV) revealed no statistically significant difference in the elasticity of testes with smaller volumes (5–10 mL) between the OA and NOA groups ($P = 0.130$), but differences in the viscosity coefficient and dispersion slope were observed ($P = 0.009$ and $P = 0.031$, respectively). The ROC curve analysis showed that the viscosity coefficient had the highest diagnostic efficacy for NOA, with an area under the curve (AUC) of 0.834. In the logistic regression, the viscosity coefficient [odds ratio (OR) = 665; 95% confidence interval (CI): 1.62–2,732.64], elasticity (OR = 1.35; 95% CI: 0.98–1.84), and TV (OR = 0.51; 95% CI: 0.44–0.61) were identified as independent risk factors for NOA.

Conclusions: The viscosity coefficient, dispersion slope, and elasticity all have diagnostic value for NOA. Unlike elasticity, the differential diagnosis of azoospermia by the viscosity coefficient and dispersion slope is not affected by TV. Testicular viscoelasticity can be effectively used in the differential diagnosis of azoospermia, especially in patients with slightly smaller testicles.

[^] ORCID: 0000-0002-8206-8361.

Keywords: Azoospermia; shear wave dispersion (SWD); shear wave elastography; testicle

Submitted Sep 14, 2024. Accepted for publication Feb 25, 2025. Published online Apr 28, 2025.

doi: 10.21037/qims-24-1944

View this article at: <https://dx.doi.org/10.21037/qims-24-1944>

Introduction

Infertility has been recognized as a public health problem by the World Health Organization (WHO), and half of the cases have been attributed to male-related factors (1-3). Ultrasound is the most frequently used non-invasive technique for examining male infertility. It is mainly used to identify the causes of infertility, such as varicocele, obstructive azoospermia (OA), and non-obstructive azoospermia (NOA) (4). Varicocele and OA have obvious ultrasound features, and can be diagnosed definitively (4), while the ultrasound images of patients with NOA may show a decrease in testicular volume (TV), or no abnormal findings (5). The differential diagnosis of azoospermia is very important because it affects the subsequent development of treatment plans (6,7). OA may be amenable to surgical or interventional correction. Conversely, treatment for NOA patients is limited to microsurgical sperm extraction paired with *in vitro* fertilization intracytoplasmic sperm injection (8-11). NOA is caused by spermatogenic failure and is accompanied by pathological changes in the testes. Thus, it is of great interest to find a new ultrasound technique that can detect these pathological changes in the testes.

Shear wave elastography (SWE) is a new elastography-based technique developed recently to obtain Young's modulus of tissue by measuring the propagation velocity of the shear wave. Young's modulus measures the stiffness of an object and is associated with the extent of fibrosis in human tissue (12). In our previous study, SWE was used for the differential diagnosis of patients with azoospermia. SWE can be used to successfully diagnose NOA; however, its diagnostic efficacy was lower than that of TV (13). Human tissue is characterized by both its elasticity and viscosity. However, the SWE technique evaluates biological tissue as a mere elastomer and ignores the effects of viscosity. Conversely, ultrasound shear wave dispersion (SWD) is a state-of-the-art technique that allows the viscosity of tissue to be assessed by calculating the dispersion slope of shear waves (14). Preliminary studies on the application of SWD imaging with convex array transducers in organs, including the liver, bile ducts, pancreas, carotid arteries, nerves, heart,

and intestines, have been conducted (15-21). However, all these studies used low-frequency convex array transducers that are suitable for examining abdominal organs but do not generate high-quality images and measurements for superficial organs. The present study was the first to use a high-frequency line array transducer-based SWD technique to detect testicular diseases in patients with infertility. This technique can reveal the details of superficial organs more accurately than techniques based on convex array low-frequency transducers, and this new SWD feature can help locate and trace regions of interest (ROIs). We present this article in accordance with the STARD reporting checklist (available at <https://qims.amegroups.com/article/view/10.21037/qims-24-1944/rc>).

Methods

Participants

The study was conducted in accordance with the Declaration of Helsinki and its subsequent amendments. The study was approved by the Ethics Committee of Renji Hospital (No. LY2023-092-B), and informed consent was obtained from all individual participants. The protocol for the research was registered on Chict.org.cn (ChiCTR2300072915).

In this prospective study, consecutive male patients with infertility who visited Renji Hospital from July 2023 to December 2023 and met the study inclusion criteria were recruited in this study. To be eligible for inclusion in the study, the patients had to meet the following inclusion criteria: (I) be able to engage in normal sexual intercourse but have been unable to achieve a clinical pregnancy for more than 1 year (in the absence of contraception); and (II) have completed a semen analysis within 7 days of the ultrasound examination. Patients were excluded from the study if they met any of the following exclusion criteria: (I) had erectile dysfunction and were incapable of engaging in sexual intercourse normally; (II) had retrograde ejaculation; (III) had a history of acute testicular and/or epididymal infection within the past month; (IV) had undergone orchiectomy or had congenital testicular absence; (V) had

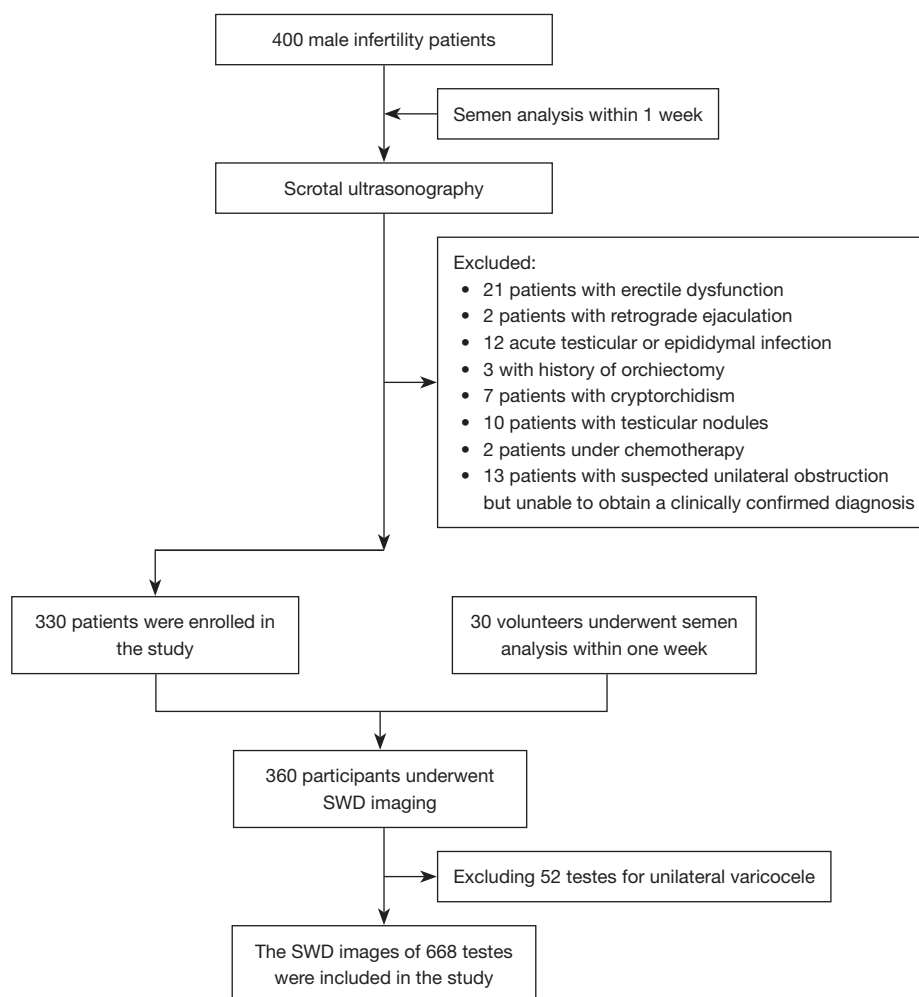


Figure 1 Flow diagram showing patient selection for this study. SWD, shear wave dispersion.

cryptorchidism and had testes that could not be detected by the SWD ultrasound probe; (VI) had a testicular mass; (VII) were undergoing radiotherapy or chemotherapy; (VIII) had azoospermia that could not be clinically diagnosed as OA or NOA; and/or (IX) had unilateral testicular obstruction or atrophy. Additionally, 30 healthy volunteers were included in the study as the control group (Figure 1).

All the enrolled patients and volunteers underwent routine scrotal ultrasonography on the bilateral testes, epididymis, vas deferens, and spermatic vein. TV was calculated using the Lambert equation, which is expressed as: $TV = \text{length} \times \text{width} \times \text{height} \times 0.71$ (22). Ultrasonography of the epididymis and vas deferens was used to aid in the assessment of OA (5). The final classification of patients with azoospermia was determined by the clinician taking the results of testicular/epididymal

sperm aspiration under consideration. Varicocele was diagnosed with ultrasound performed per the recommendations of the European Society of Urogenital Radiology Scrotal and Penile Imaging Working Group by measuring the internal diameters and reflux time of the spermatic vein in the standing position (23,24). Based on these findings, all patients were assigned to one of the following four groups: the ultrasound normal group, the varicocele group, the NOA group, and the OA group. The ultrasound normal group was further divided into two subgroups: the ultrasound normal I group (comprising patients with normal ultrasound and semen analysis results) and the ultrasound normal II group [comprising patients with normal ultrasound results but a sperm concentration (SC) $<15 \times 10^6/\text{mL}$ or progressive motility $<32\%$ or morphology $<4\%$].

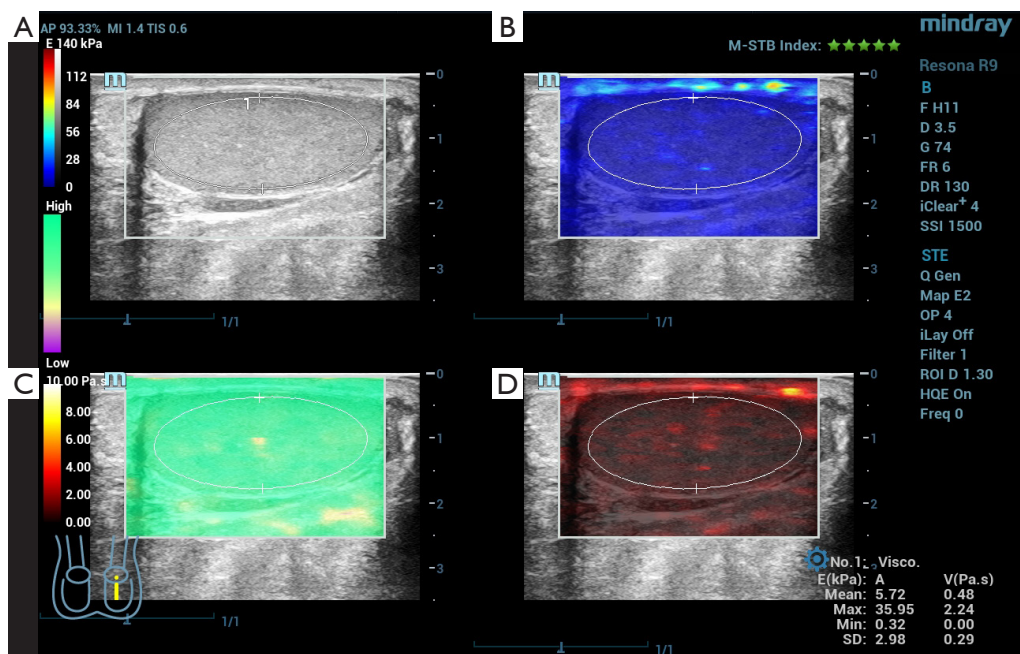


Figure 2 Shear wave dispersion imaging of a testicle. An elliptical ROI containing as much of the testicular tissue as possible while excluding the tunica albuginea of the testis. (A) B-mode map. (B) Shear wave elastography map. (C) Confidence-level map. (D) Shear wave dispersion map. ROI, region of interest.

Ultrasound and SWD imaging protocol for participants

All the patients and volunteers underwent SWD imaging of the testes using a Resona 9-s color Doppler diagnostic ultrasound system equipped with an 8–15-MHz line array transducer (Mindray Bio-Medical Electronics, Shenzhen, China). All the ultrasound examinations and SWD imaging were performed by two physicians with over 10 years of experience each in andrology ultrasound. The patients were examined in a supine position with their scrotums exposed. The patients were instructed to breathe calmly and remain still, and the largest longitudinal ultrasound section of each testis was selected under the gray-scale mode, and imaged with the SWD mode. After clicking on the SWD imaging start button, an SWD image was acquired about 4 s later. If the confidence level of the image reached 90% or higher, the image was saved in the diagnostic ultrasound system database for further analysis. Next, the largest transverse ultrasound section of each testis was selected using the two-dimensional ultrasound mode, and SWD imaging was initiated with the images saved as described above. Both testes of each patient were measured five times; viscoelasticity images were acquired and saved, with information on SWE, SWD, and the image confidence level included on each image. An elliptical ROI containing as

much of the testicular tissue as possible while excluding the tunica albuginea of the testis was drawn for the image analysis. The SWE imaging provided measurements of elasticity, while the SWD imaging provided measurements of the viscosity coefficient and dispersion slope. The maximum, minimum, and mean values of each measurement were recorded on the images, and the mean values were further recorded and saved (Figure 2). Each testis was measured five times following the steps mentioned above, and the median value was recorded for further data analysis.

Semen analysis

All the patients underwent semen analysis within 1 week of the ultrasound examination. The semen analysis was performed as per the instructions in the 2021 WHO manual, 6th edition (25), with parameters including SC, motility, and morphology recorded. If no sperm were found in the semen, another two semen analyses were performed to confirm azoospermia.

Statistical analysis

The statistical analysis was performed using SPSS 20.0

Table 1 Viscoelasticity in different disease groups

Variables	Volunteers	US normal I	US normal II	Varicocele	NOA	OA	P
N	60	102	192	216	58	40	
Age (years)	31.48±6.83	33.65±8.5	34.12±7.41	32.93±5.58	33.25±5.21	36.46±12.65	0.077
TV (mL)	15.01±4.15	14.95±3.56	14.27±4.14	14.36±3.71	6.78±4.77 [†]	14.57±3.76	<0.001
SC (×10 ⁶ /mL)	19.11±9.14	18.41±10.83	11.94±12.73	9.36±8.27	0	0	<0.001
Motility (%)	38.21±12.1	39.16±13.74	22.38±11.57	26.54±14.38	–	–	<0.001
Morphology (%)	4.87±1.43	4.96±1.59	3.64±1.43	3.37±1.16	–	–	<0.001
Viscosity coefficient (Pa·s)	0.51±0.12	0.52±0.11	0.53±0.14	0.53±0.12	0.71±0.15 [†]	0.56±0.14	<0.001
Dispersion slope (m/s/kHz)	1.48±0.49	1.44±0.42	1.47±0.51	1.51±0.45	1.88±0.64 [†]	1.62±0.52	<0.001
Elasticity (kPa)	6.61±1.98	6.47±1.26	6.49±1.63	6.71±1.55	9.59±3.70 [†]	6.84±1.48	<0.001

Data are presented as the mean ± standard deviation, or as the number of testes. [†], compared with other groups using the *t*-test, the difference was statistically significant (*P*<0.05). N, number of testes; NOA, non-obstructive azoospermia; OA, obstructive azoospermia; SC, sperm concentration; TV, testicular volume; US, ultrasound; US normal I, patients with normal ultrasound and semen analysis results; US normal II, patients with normal ultrasound results sperm concentration <15×10⁶/mL or progressive motility <32% or morphology <4%.

software (IBM SPSS Statistics, RRID:SCR_016479). The inter-reader variability between the two physicians was assessed. Data obtained from the longitudinal and transverse sections of the testes were compared using a paired *t*-test. A one-way analysis of variance (ANOVA) was used for comparisons between groups with different diseases, and Bonferroni correction was used for the multi-group comparisons. The correlation between two variables was examined using the bivariate Pearson correlation analysis. The diagnostic efficacy of viscoelasticity was evaluated by receiver operating characteristic (ROC) curve analysis. Binary logistic regression was used to analyze the risk factors for NOA. A *P* value <0.05 was considered statistically significant.

Results

Participant characteristics

A total of 330 patients and 30 healthy volunteers were included in the study, and a total of 720 testes underwent SWD imaging. *Figure 1* shows the number of participants excluded based on each exclusion criterion. The number of patients in the ultrasound normal group I, ultrasound normal group II, the varicocele group, the NOA group, and the OA group were 51 (15.5%), 96 (29.1%), 134 (40.6%), 82 bilateral varicocele and 52 unilateral varicocele), 29 (8.8%) and 20 (6.1%), respectively. The statistical

analysis was conducted on a single testicle basis, and for the patients with unilateral varicocele, only the testes on the affected side were assessed (*Table 1*).

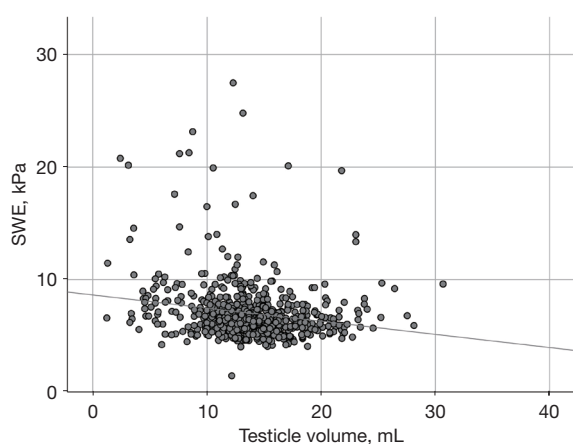
SWD and SWE imaging analysis

In terms of the inter-observer agreement of the two physicians, the intraclass correlation coefficient (ICC) values of the viscosity coefficient, dispersion slope, and elasticity were 0.920 [95% confidence interval (CI): 0.764–0.964], 0.958 (95% CI: 0.931–0.975), and 0.869 (95% CI: 0.505–0.948), respectively, indicating excellent reliability. The SWE and SWD imaging-derived measurements obtained from the transverse and longitudinal sections are shown in *Table 2*. The viscosity coefficient, dispersion slope, and elasticity did not differ significantly between the transverse and longitudinal sections (*P*>0.05). The number of patients and volunteers in each group and the corresponding SWE and SWD imaging-derived measurements are shown in *Table 1*. The ANOVA results showed that the differences in the TV, viscosity coefficient, dispersion slope, and elasticity among the different disease groups were statistically significant. After multi-group comparisons, the NOA group was found to have higher viscosity and elasticity but a smaller TV than the other disease groups (*P*<0.05). There was no statistically significant difference between the volunteer group, ultrasound normal I group, ultrasound normal II group, varicocele group, and OA group. Elasticity

Table 2 SWE and SWD measurements from the transverse and longitudinal sections

Viscoelasticity	N	Longitudinal	Transverse	P
SWD (viscosity coefficient) (Pa-s)	608	0.54±0.13	0.54±0.15	0.942
US normal	294	0.52±0.11	0.54±0.14	
Varicocele	216	0.53±0.12	0.51±0.14	
NOA	58	0.71±0.15	0.68±0.15	
OA	40	0.56±0.14	0.61±0.25	
SWD (dispersion slope) (m/s/kHz)	608	1.51±0.47	1.48±0.54	0.315
US normal	294	1.44±0.42	1.46±0.52	
Varicocele	216	1.51±0.45	1.40±0.44	
NOA	58	1.88±0.64	1.85±0.68	
OA	40	1.62±0.52	1.68±0.68	
SWE (elasticity) (kPa)	608	6.84±1.90	6.89±2.59	0.475
US normal	294	6.47±1.26	6.64±1.74	
Varicocele	216	6.71±1.55	6.62±2.08	
NOA	58	9.59±3.70	9.47±1.84	
OA	40	6.84±1.48	6.85±1.87	

Data are presented as the mean ± standard deviation, or as the number of testes. N, number of testes; NOA, non-obstructive azoospermia; OA, obstructive azoospermia; SWD, shear wave dispersion; SWE, shear wave elastography; US, ultrasound.

**Figure 3** The relationship between the elasticity and testicular volume. SWE, shear wave elastography.

was negatively correlated with TV ($r=-0.201$), while the viscosity coefficient and dispersion slope were not correlated with TV (*Figure 3*). Comparisons of these characteristic measurements of SWD and SWE imaging in the different disease groups after subgrouping by TV are shown in *Figure 4*. Except for a limited number of patients with a TV

of 0–5 mL, the viscosity coefficient and dispersion slope of the testes with different TVs were all significantly higher in the NOA group than the other disease groups. However, in relation to testicular elasticity, no statistically significant difference was found between the patients with NOA and OA who had a TV of 5–10 mL ($P>0.05$). Thus, based on the results, SWE was not capable of distinguishing between OA and NOA in patients with a TV <10 mL, but the measurements derived from SWD imaging could be used to distinguish between such patients.

ROC curve and logistic regression analyses of viscoelasticity

A ROC curve analysis was conducted to evaluate the diagnostic values of the viscosity coefficient, dispersion slope, and elasticity for NOA (*Table 3*). The viscosity coefficient had the best diagnostic efficacy with an area under the curve (AUC) of 0.834. When the cut-off value was set to 0.615 Pa-s, the corresponding sensitivity and specificity were 81.8% and 79.5%, respectively. In logistic regression, the viscosity coefficient [odds ratio (OR) =665; 95% CI: 1.62–2,732.64], elasticity (OR =1.35; 95% CI: 0.98–1.84), and TV (OR =0.51; 95% CI: 0.44–0.61) were

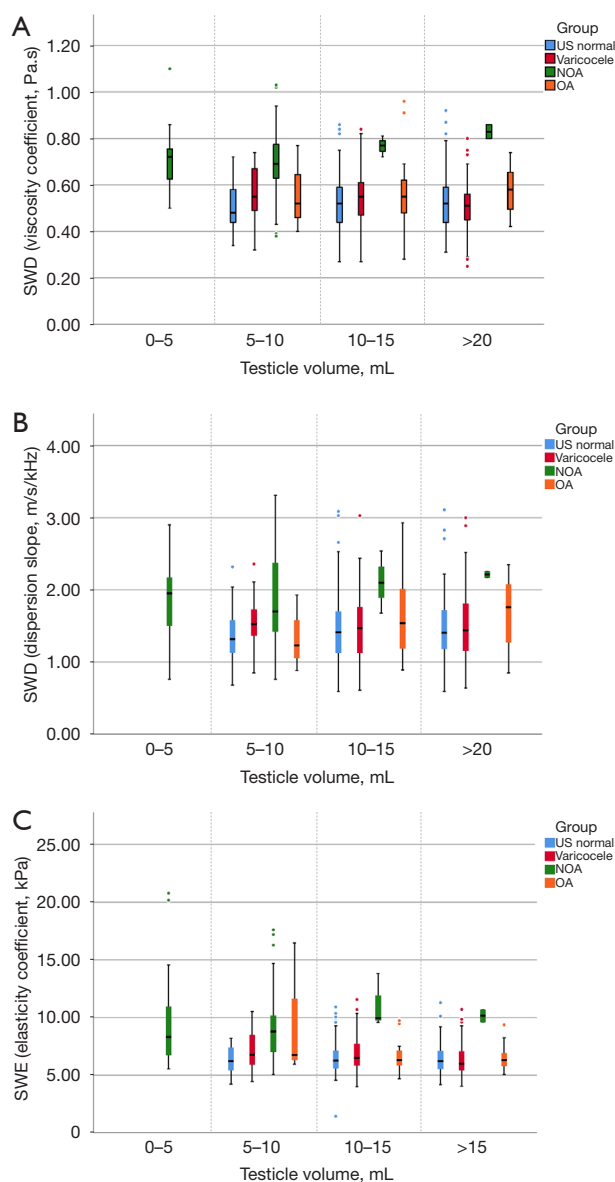


Figure 4 Testicular viscoelasticity of different disease groups based on testicular volume subgrouping. (A) Viscosity coefficient. (B) Dispersion slope. (C) Elasticity. NOA, non-obstructive azoospermia; OA, obstructive azoospermia; SWD, shear wave dispersion; SWE, shear wave elastography; US, ultrasound.

identified as independent risk factors for NOA.

Discussion

SWD imaging is the latest technique for viscosity assessment. It determines tissue viscosity by comparing the slope calculated from the curve of the shear wave frequency to the speed. SWD imaging-derived information has been found to be associated with pathological changes, such as tissue necrosis, inflammation, and fatty infiltration, but it is more weakly associated with fibrosis than SWE-derived information (15-21). In our study, we found that the SWD imaging-derived parameters had better stability than the SWE-imaging-derived parameters. This means that viscoelasticity can efficiently and accurately measure tissue viscosity without the need for excessive repeated measurements. Standard sections are easier to obtain longitudinally than transversely; thus, all of the analyses in this study were conducted using longitudinal sections. When comparing the different disease groups, the SWE and SWD imaging-derived measurements were significantly different in the NOA group than the other disease groups; however, the differences among the other disease groups were not statistically significant. The increased testicular viscoelasticity can be attributed to the presence of pathological changes, such as atrophy, seminiferous tubule collapse, and testicular tissue hyalinization, in the testes of patients with NOA. The patients in the other groups might have had comprised spermatogenic function, but as no significant changes were observed in the structure of the seminiferous tubules, no significant changes in viscoelasticity were detected.

In addition to higher viscoelasticity, the NOA group had a smaller TV than the other groups. To investigate whether the increased testicular viscoelasticity in patients with NOA is due to their small TVs, we analyzed the correlations between measurements derived from SWE imaging, SWD imaging, and TV. Testicular elasticity was found to be negatively correlated with TV, while the viscosity coefficient and dispersion slope were not correlated with TV. Cui *et al.*

Table 3 Differential diagnosis of NOA with ROC curves

Viscoelasticity	AUC	95% CI	Cut-off value	Sensitivity (%)	Specificity (%)	P
Viscosity coefficient	0.834	0.769–0.902	0.615	81.8	79.5	<0.001
Dispersion slope	0.695	0.613–0.780	1.585	70.9	63.8	<0.001
Elasticity	0.796	0.726–0.864	7.115	72.7	72.5	<0.001

AUC, area under the curve; CI, confidence interval; NOA, non-obstructive azoospermia; ROC, receiver operating characteristic.

analyzed testicular elasticity obtained from SWE in 1,116 patients and volunteers, and found statistically significant differences between the NOA group and all other disease groups (26,27). Shin *et al.* examined the relationships between age, weight, TV, and shear wave velocity in pediatric patients, and found that TV increased while shear wave velocity decreased as the children aged (28). These findings confirmed the negative correlation between TV and the SWE-derived parameters. Noting that the results obtained from the normal testes of pediatric patients were similar to our SWE results obtained from the testes of patients with infertility, we hypothesized that TV critically affects the magnitude of SWE-derived measurements. The tunica albuginea of the testis, a tissue with a predominantly fibrous component and high surface tension, might have contributed to the increased shear wave elasticity in the surrounding tissue. Trottmann *et al.* (29) studied the shear wave elasticity of the normal human testis, and found that the elasticity was higher in the upper and lower testicular regions than the middle region. The ROIs for testes with smaller volumes tend to contain more tissue close to the tunica albuginea, resulting in elevated shear wave elasticity. We sub-grouped the testes according to their sizes and found that all the patients with a TV of 0–5 mL belonged to the NOA group. Thus, the effect of a small testicular size could not be compared statistically in our data set. The viscoelasticity measurements for testes sized 0–5 mL did not differ from those of other sizes. In the remaining groups, we found that the magnitude of the SWE-derived measurements increased in the patients with OA as the TV decreased. Among the patients with a TV of 5–10 mL, the SWE-derived measurements were not capable of distinguishing between the patients with NOA and OA. Additionally, the SWD imaging-derived measurements had the same efficacy in distinguishing between the types of azoospermia in all patients with different TVs. We believe that the advantage of using SWD imaging is that the measurements are independent of TV. Therefore, SWD imaging can identify NOA even in small testes. Conversely, SWE is affected by testicular size in identifying NOA. This difference may be due to the distinct principles underlying SWE and SWD imaging. Specifically, SWE detects the propagation velocity of shear waves that is higher in the tissue near the tunica albuginea due to its greater surface tension. Meanwhile, SWD imaging measures the ratio of velocity changes that is not affected by the shear wave velocity at a single frequency. Indeed, TV may be one reason for the elevated testicular shear wave elasticity in patients. However, pathological changes in the testis are the main factor

affecting shear wave elasticity. Notably, we found that the elevated elasticity was not as pronounced in the ultrasound of the normal patients and those with varicocele who had a TV of 5–10 mL.

The ROC curve and logistic regression analyses revealed that the viscosity coefficient had the best diagnostic efficacy in the differential diagnosis of azoospermia. Although the viscosity coefficient and the dispersion slope are both SWD imaging-derived measurements, they are not linearly correlated and thus have divergent applications in clinical practice. We also noted that the viscosity coefficient had better repeatability than the dispersion slope during the examinations, indicating that the diagnostic efficacy of the two indices differ. Conversely, while the diagnostic efficacy of SWE was influenced by a small TV, the effect was limited, as few patients with OA had a TV <10 mL.

Our study had some limitations. First, the number of azoospermia patients, especially OA patients with a TV <10 mL, was relatively low compared to the number of patients with normal ultrasound results and varicocele. This limitation may affect the accuracy of viscoelasticity for OA in small testes using the proposed technique. We intend to address this sample size deficiency in future studies.

Conclusions

The viscosity coefficient, dispersion slope, and elasticity of testes can be used in the diagnosis of NOA but are not useful in the diagnosis of varicocele and OA. The efficacy of diagnosing NOA by elasticity is affected by TV and is reduced in patients with a TV <10 mL. The diagnostic efficacy of the viscosity coefficient and dispersion slope for NOA is not affected by TV. Testicular viscoelasticity can be effectively used in the differential diagnosis of azoospermia, especially in patients with slightly smaller testicles. The viscosity coefficient has the best diagnostic efficacy among all parameters derived from testicular viscoelasticity.

Acknowledgments

The authors are especially grateful to all their colleagues who helped them to conduct the study and collect the study data. The authors would also like to thank the Shanghai Institute of Andrology for their assistance with this study.

Footnote

Reporting Checklist: The authors have completed the STARD

reporting checklist. Available at <https://qims.amegroups.com/article/view/10.21037/qims-24-1944/rc>

Funding: The work was supported by the National Natural Science Foundation of China (No. 82171936), and the Clinical Research Initiative of the Shanghai Municipal Health Commission (project No. 202140451).

Conflicts of Interest: All authors have completed the ICMJE uniform disclosure form (available at <https://qims.amegroups.com/article/view/10.21037/qims-24-1944/coif>). The authors have no conflicts of interest to declare.

Ethical Statement: The authors are accountable for all aspects of the work in ensuring that questions related to the accuracy or integrity of any part of the work are appropriately investigated and resolved. The study was conducted in accordance with the Declaration of Helsinki and its subsequent amendments. The study was approved by the Ethics Committee of Renji Hospital (No. LY2023-092-B), and informed consent was obtained from all individual participants.

Open Access Statement: This is an Open Access article distributed in accordance with the Creative Commons Attribution-NonCommercial-NoDerivs 4.0 International License (CC BY-NC-ND 4.0), which permits the non-commercial replication and distribution of the article with the strict proviso that no changes or edits are made and the original work is properly cited (including links to both the formal publication through the relevant DOI and the license). See: <https://creativecommons.org/licenses/by-nc-nd/4.0/>.

References

1. Lotti F, Maggi M. Sexual dysfunction and male infertility. *Nat Rev Urol* 2018;15:287-307.
2. Andrade DL, Viana MC, Esteves SC. Differential Diagnosis of Azoospermia in Men with Infertility. *J Clin Med* 2021;10:3144.
3. Medenica S, Zivanovic D, Batkoska L, Marinelli S, Basile G, Perino A, Cucinella G, Gullo G, Zaami S. The Future Is Coming: Artificial Intelligence in the Treatment of Infertility Could Improve Assisted Reproduction Outcomes-The Value of Regulatory Frameworks. *Diagnostics (Basel)* 2022;12:2979.
4. Mittal PK, Little B, Harri PA, Miller FH, Alexander LF, Kalb B, Camacho JC, Master V, Hartman M, Moreno CC. Role of Imaging in the Evaluation of Male Infertility. *Radiographics* 2017;37:837-54.
5. Du J, Li FH, Guo YF, Yang LM, Zheng JF, Chen B, Zhu JS, Liu Q. Differential diagnosis of azoospermia and etiologic classification of obstructive azoospermia: role of scrotal and transrectal US. *Radiology* 2010;256:493-503.
6. Olesen IA, Andersson AM, Aksglaede L, Skakkebaek NE, Rajpert-de Meyts E, Joergensen N, Juul A. Clinical, genetic, biochemical, and testicular biopsy findings among 1,213 men evaluated for infertility. *Fertil Steril* 2017;107:74-82.e7.
7. Gullo G, Basile G, Cucinella G, Greco ME, Perino A, Chiantera V, Marinelli S. Fresh vs. frozen embryo transfer in assisted reproductive techniques: a single center retrospective cohort study and ethical-legal implications. *Eur Rev Med Pharmacol Sci* 2023;27:6809-23.
8. Gullo G, Scaglione M, Buzzaccarini G, Laganà AS, Basile G, Chiantera V, Cucinella G, Zaami S. Cell-Free Fetal DNA and Non-Invasive Prenatal Diagnosis of Chromosomopathies and Pediatric Monogenic Diseases: A Critical Appraisal and Medicolegal Remarks. *J Pers Med* 2022;13:1.
9. Gullo G, Scaglione M, Cucinella G, Chiantera V, Perino A, Greco ME, Laganà AS, Marinelli E, Basile G, Zaami S. Neonatal Outcomes and Long-Term Follow-Up of Children Born from Frozen Embryo, a Narrative Review of Latest Research Findings. *Medicina (Kaunas)* 2022;58:1218.
10. Gullo G, Scaglione M, Cucinella G, Perino A, Chiantera V, D'Anna R, Laganà AS, Buzzaccarini G. Impact of assisted reproduction techniques on the neuro-psychomotor outcome of newborns: a critical appraisal. *J Obstet Gynaecol* 2022;42:2583-7.
11. Burgio S, Polizzi C, Buzzaccarini G, Laganà AS, Gullo G, Perricone G, Perino A, Cucinella G, Alesi M. Psychological variables in medically assisted reproduction: a systematic review. *Prz Menopauzalny* 2022;21:47-63.
12. Herrmann E, de Lédinghen V, Cassinotto C, Chu WC, Leung VY, Ferraioli G, et al. Assessment of biopsy-proven liver fibrosis by two-dimensional shear wave elastography: An individual patient data-based meta-analysis. *Hepatology* 2018;67:260-72.
13. Li X, Tian RH, Li P, Li CX, Yao MH, Yao CC, Wang XB, Jiang LR, Li Z, Wu R. Ultrasonographic evaluation of the rete testis thickness: a promising approach to differentiate obstructive from nonobstructive azoospermia. *Asian J Androl* 2023;25:725-30.
14. Schulz M, Kleinjans M, Strnad P, Demir M, Holtmann

- TM, Tacke F, Wree A. Shear Wave Elastography and Shear Wave Dispersion Imaging in the Assessment of Liver Disease in Alpha1-Antitrypsin Deficiency. *Diagnostics (Basel)* 2021;11:629.
15. Sugimoto K, Moriyasu F, Oshiro H, Takeuchi H, Yoshimasu Y, Kasai Y, Itoi T. Clinical utilization of shear wave dispersion imaging in diffuse liver disease. *Ultrasonography* 2020;39:3-10.
 16. Schulz M, Wilde AB, Demir M, Müller T, Tacke F, Wree A. Shear wave elastography and shear wave dispersion imaging in primary biliary cholangitis-a pilot study. *Quant Imaging Med Surg* 2022;12:1235-42.
 17. Suzuki H, Ishikawa T, Ohno E, Iida T, Uetsuki K, Yashika J, Yamada K, Yoshikawa M, Furukawa K, Nakamura M, Honda T, Ishigami M, Kawashima H, Fujishiro M. An initial trial of quantitative evaluation of autoimmune pancreatitis using shear wave elastography and shear wave dispersion in transabdominal ultrasound. *Pancreatology* 2021;21:682-7.
 18. Luo X, Du L, Li Z. Ultrasound assessment of tensile stress in carotid arteries of healthy human subjects with varying age. *BMC Med Imaging* 2019;19:93.
 19. Liu F, Li D, Xin Y, Liu F, Li W, Zhu J. Quantification of Nerve Viscosity Using Shear Wave Dispersion Imaging in Diabetic Rats: A Novel Technique for Evaluating Diabetic Neuropathy. *Korean J Radiol* 2022;23:237-45.
 20. Amioka N, Takaya Y, Nakamura K, Kondo M, Akazawa K, Ohno Y, Ichikawa K, Nakayama R, Saito Y, Akagi S, Miyoshi T, Yoshida M, Morita H, Ito H. Impact of shear wave dispersion slope analysis for assessing the severity of myocarditis. *Sci Rep* 2022;12:8776.
 21. Yamada K, Ishikawa T, Kawashima H, Ohno E, Iida T, Ishikawa E, Mizutani Y, Sawada T, Maeda K, Yamamura T, Kakushima N, Furukawa K, Nakamura M, Ishigami M, Fujishiro M. Evaluation of ulcerative colitis activity using transabdominal ultrasound shear wave elastography. *Quant Imaging Med Surg* 2022;12:618-26.
 22. Hsieh ML, Huang ST, Huang HC, Chen Y, Hsu YC. The reliability of ultrasonographic measurements for testicular volume assessment: comparison of three common formulas with true testicular volume. *Asian J Androl* 2009;11:261-5.
 23. Bertolotto M, Freeman S, Richenberg J, Belfield J, Dogra V, Huang DY, et al. Ultrasound evaluation of varicoceles: systematic literature review and rationale of the ESUR-SPIWG Guidelines and Recommendations. *J Ultrasound* 2020;23:487-507.
 24. Freeman S, Bertolotto M, Richenberg J, Belfield J, Dogra V, Huang DY, et al. Ultrasound evaluation of varicoceles: guidelines and recommendations of the European Society of Urogenital Radiology Scrotal and Penile Imaging Working Group (ESUR-SPIWG) for detection, classification, and grading. *Eur Radiol* 2020;30:11-25.
 25. Esteves SC. Evolution of the World Health Organization semen analysis manual: where are we? *Nat Rev Urol* 2022;19:439-46.
 26. Cui J, Du Q, Fu W. Application of real-time shear wave elastography in the assessment of male infertility. *Quant Imaging Med Surg* 2022;12:1505-16.
 27. Fu W, Cui J, Tang S. The role of testicular stiffness derived from shear wave elastography in the assessment of spermatogenesis in men with varicocele. *Quant Imaging Med Surg* 2024;14:4987-97.
 28. Shin HJ, Yoon H, Lee YS, Kim MJ, Han SW, Roh YH, Lee MJ. Normal Changes and Ranges of Pediatric Testicular Volume and Shear Wave Elasticity. *Ultrasound Med Biol* 2019;45:1638-43.
 29. Trottmann M, Marcon J, D'Anastasi M, Bruce MF, Stief CG, Reiser MF, Buchner A, Clevert DA. Shear-wave elastography of the testis in the healthy man - determination of standard values. *Clin Hemorheol Microcirc* 2016;62:273-81.

Cite this article as: Zhang S, Wu M, Xu L, Wang H, Jiang L. High-frequency ultrasound shear wave dispersion imaging for male infertility: a pilot study. *Quant Imaging Med Surg* 2025;15(5):4286-4295. doi: 10.21037/qims-24-1944